ELECTRON INSTABILITIES IN HALL THRUSTERS: MODELING AND APPLICATION TO ELECTRIC FIELD DIAGNOSTICS

A. Kapulkin*, J. Ashkenazy, A. Kogan*, G. Appelbaum**, D. Alkalay*, M.Guelman***

* Asher Space Research Institute, Technion, I.I.T., Haifa, 32000, Israel
** Propulsion Physics Laboratory, Soreq, NRC, Yavne 81800, Israel
E-mail: Alexander Kapulkin kapulkin@tx.technion.ac.il
Joseph Ashkenazy joseph@soreq.gov.il

Abstract

The paper is devoted to a theoretical analysis of large-scale electron instabilities in Hall thrusters (HT), the spectrum of which resides mainly in the megahertz range. Numerical and analytical methods in the collisionless MHD approximation were used. Two kinds of oscillations: Rayleigh type perturbations and Doppler shifted electron gradient waves have been identified as unstable. The first of them are unstable in linear approximation, the second can be excited as a result of non-linear three waves interaction. It was found that the Rayleigh type instability smoothes the profile of the longitudinal electric field. This instability can be the main factor that limits effectively the electric field in the channel. The electron instabilities in HT can be used for diagnostics of the electric field distribution in the thruster. The approach to validate experimentally the theoretical model of electron perturbations in HT is discussed also.

1. Introduction

During last years the investigations of Hall thrusters working processes entered qualitatively a new stage, which is related to the wide application of computer modeling. Nevertheless, the general state of understanding of wave processes details is still not satisfactory. It is still not clear, what is the role of the wave processes in forming such important parameter as the electric field distribution in the channel, which determines the ion plume angular divergence, and finally the thruster lifetime. What is the reason of the rather broad spectrum of oscillations in HT – the energy transfer in spectrum from several unstable modes, due to non-linear processes, or the large amount of unstable modes itself? In the present work we focus our attention on the investigation of relatively large-scale electron perturbations in the thruster. The choice of the object of investigation was dictated by the following considerations: 1) these oscillations have relatively high amplitude; 2) there is strong reason to think that they influence the limiting value of the electric field in the thruster (see paragraph 3); 3) since mainly electrons are involved in these oscillations, the theoretical consideration of perturbations becomes simpler, which allows to advance further in the creation of a realistic model of these oscillations.

The early investigations of electron perturbations in Hall thrusters are described in [1, 2]. Later they were continued in [3-5]. In these investigations MHz range oscillations were experimentally found, which look like peaks on the background of a more continuous spectrum. It was shown, that the electron drift velocity non-uniformity might be responsible for their excitation. The present paper is in part the development of the work described in [5] In contrast to [5], devoted mainly to the possible application of a specific type of electron perturbations for non-contact electric field diagnostics, here more attention is paid to the analysis of mechanisms of electron perturbations excitation and influence of the electron instability on the processes in HT. The numerical scheme improvement in comparison with the scheme applied in [5], allowed to advance in the direction of more realistic (more sharp) profiles of undisturbed parameters in the thruster that in turn allowed to improve significantly the understanding of factors, which define the structure of electron perturbations spectrum, and to indicate the way for suppressing the electron instability. In this work the possible ways for experimental validation of the theoretical model are also discussed.

2. Theoretical Model

The investigations were carried out in the frames of the electron non-collisional MHD. Electrons are assumed to be cold. Ions are not involved in oscillations. They create the neutralizing background in non-disturbed state. Neglect of the ion dynamics became possible since in the perturbations under consideration we have: 1) $\omega >> \sqrt{\omega_{iB}\omega_{eB}}, k_x V_0$, where

$\omega_{Bi}=eB_0/m_i$ - ion gyrofrequency,

$\omega_{Be}=eB_0/m_e$ - electron gyrofrequency,
e – unit positive electric charge,
B_0 – magnetic field induction,
m_i, m_e – ion and electron mass correspondingly,
V_0 – average ion velocity in the channel,
k_x – the component of wave vector directed along the applied electric field;

2)

$$\frac{\omega_{pi}^2}{\omega_{pe}^2} << \left[\frac{\omega}{\omega_{Be}}\right]^2, \qquad (1)$$

where $\omega_{pi} = e\sqrt{\frac{n_0}{\varepsilon_0 m_i}}$, $\omega_{pe} = e\sqrt{\frac{n_0}{\varepsilon_0 m_e}}$ - ion and electron Langmuir frequencies correspondingly,

n_o – undisturbed electron (ion) number density
ε_0 – vacuum dielectric permittivity.

The oscillations are supposed to be potential, since we consider perturbations such that

$$\frac{k_\Sigma B_0}{\sqrt{\mu_0 m_i n_0}} << \omega << \frac{k_\Sigma B_0}{\sqrt{\mu_0 m_e n_0}}, \qquad \frac{\omega^2}{k^2 c^2} << 1.$$

Where k_Σ is total wave number, c velocity of light in vacuum, μ_0 magnetic permittivity.

We suppose that the wave phase does not change significantly along the magnetic field. We chose the following coordinate system: X axis is directed along the electric field, Z axis is directed along the magnetic field. In this case electrons in undisturbed state drift along the Y axis with the velocity of $u_0=-E_0/B_0$ where E_0 is undisturbed electric field.

Using these assumptions, the linearized system of electron magnetohydrodynamics is:

$$\begin{aligned}
&\frac{\partial \mathbf{u}}{\partial t} + (\mathbf{u}_0\nabla)\mathbf{u} + (\mathbf{u}\nabla)\mathbf{u}_0 = \frac{e}{m_e}\nabla\Phi - \frac{e}{m_e}\mathbf{u}\times\mathbf{B}_0 \\
&\frac{\partial n}{\partial t} + div(n\mathbf{u}_0 + n_0\mathbf{u}) = 0 \qquad (2) \\
&\Delta\Phi = \frac{en}{\varepsilon_0}
\end{aligned}$$

where $\mathbf{u}$ – electron velocity perturbations,
n – electron number density perturbations.

The values with the "0" subscript are undisturbed. We can seek the solution of the system (2) as $\mathbf{F}(x,y,t) = \mathbf{F}_k(x)\exp(-i(\omega t - ky))$, where $\mathbf{F} = (u_x, u_y, n, \Phi)^T; \mathbf{F}_k = (u_{kx}, u_{ky}, n_k, \Phi_k)^T$.

The values with "k" subscript are Fourier-components of the corresponding parameters. k – the wave vector projection on Y axis (in the real ring geometry $k=m/r_0$, where $m=\pm1$, ±2 …. - azimuth wave number, r_0 is the acceleration channel average radius).

In this case, considering the electron inertia only in first approximation relative to

$$\frac{|\omega|}{\omega_{Be}} \sim \frac{|ku_0|}{\omega_{Be}} \sim \frac{1}{\omega_{Be}}\left|\frac{\partial u_0}{\partial x}\right| \qquad (3)\ *,$$

and taking into account, that in HT the condition

$$\frac{\omega_{pe}^2}{\omega_{Be}^2} >> 1 \qquad (4)$$

holds, we obtain the following equation for the electric potential Fourier-component:

*There is no contradiction with (1), while we neglect the square of the ratio ω/ω_{Be} in comparison with 1 , because in the case of xenon plasma the left side of (1) is of the order of 10^{-5}, and therefore that condition is easily satisfied.

$$\frac{d^2\Phi_k}{dx^2}+\frac{d}{dx}(\ln\frac{n_0}{B_0^2})\frac{d\Phi_k}{dx}+\Big[\frac{k\omega_{Be}}{\omega-ku_0}\frac{d}{dx}(\ln\frac{n_0}{B_0})+\frac{k}{\omega-ku_0}\frac{du_0}{dx}\frac{d}{dx}\left(\ln\frac{n_0}{B_0^2}\right)+\frac{k}{\omega-ku_0}\frac{d^2u_0}{dx^2}-k^2\Big]\Phi_k=0 \quad (5)$$

It is logical to use as boundary conditions

$$\Phi_k(0)=\Phi_k(d)=0 \quad (5'),$$

where d is the distance between the anode and conditional cathode.

If $n_0=const$ and $B_0=const$, equation (5) reduces to Rayleigh's equation:

$$\frac{d^2\Phi_k}{dx^2}-k^2\Phi_k+\frac{k}{\omega-ku_0}\frac{d^2u_0}{dx^2}\Phi_k=0 \quad (6)$$

Equation (6) describes the stability of ideal fluid flow with the lateral flow velocity non-uniformity. The necessary condition of instability is the presence of at least one point of inflection in the velocity profile. This instability is called Rayleigh instability. If the velocity profile is step function, it is more known as Kelvin-Helmholtz instability. The same equation describes diocotron instability of purely electron plasma. It is worth mentioning that in the case of diocotron instability equation (6) describes the perturbations of the electron number density during their inertia-free motion, and is obtained upon the opposite condition to (4). In our case equation (6) describes the perturbations of electron velocity and potential without change in their number density.

In [3-5] it was shown that the electron perturbations instability described by equation (6) in the case of a Hall thruster is a strong instability. The instability increment is of the same order as the drift frequency $(\omega\sim kU_0)$.

3. Influence of Rayleigh Electron Perturbation Instability on Thruster Processes

Before discussing the possible influence of the Rayleigh instability on the HT processes, let's consider the relevancy of the electron perturbations analysis on the basis of the equation (6), which was derived for the case $n_0=const$ and $B_0=const$. In Fig. 1, the typical distributions of electric and magnetic field, and electron number density in thrusters are presented in non-dimensional form. As it is seen from the figure, there are two significantly different in special scale, non-uniformities of parameters. One is for electric field or drift velocity, let's designate it δ, the other is for magnetic field and electron number density, let's designate it L. Since δ is significantly lower than L, it seems to give a possibility to neglect the n_0 and B_0 gradients during the consideration of the Rayleigh instability. But because of the presence of the very large factor ω_{Be}, the situation for the third term in equation (5) is significantly more difficult. The condition of admissibility of equation (6) is given by,

$$\alpha=\left|\frac{\omega_{Be}\delta^2}{Lu_{0\max}}\right|<<1 \quad (7),$$

where $L=\left|\frac{d}{dx}\left(\ln\frac{n_0}{B_0}\right)\right|^{-1}$, $u_{0\max}$-maximum value of u_0 in the channel.

The non-dimensional parameter α is the ratio of the third and fifth terms of equation (5). For $B_0=1.4\cdot10^{-2}$ T; $E_0=1.64\cdot10^4$ V/m; $\delta=3\cdot10^{-3}$ m; $L=3.5\cdot10^{-2}$ m, $\alpha=0.54$, which, apparently, does not fully correspond to condition (7), but nevertheless some qualitative conclusions concerning the properties of Rayleigh perturbations in HT are still possible to derive on the basis of equation (6).

Let's begin nevertheless from the general note, concerning all purely electron perturbations, including those described by the full equation (5). Since ions are not involved in the described perturbations, the development of instabilities should not be accompanied by enhanced electron current across the magnetic field, owing to the momentum conservation law. Then the question arises: since Rayleigh instability can not cause enhanced electron current, maybe it is "harmless" and does not negatively influence the thruster characteristics. Unfortunately, it seems not correct because of the following reason. During this instability, the increment increases upon the increase of the second derivative of the drift velocity. It gives us reasons to think that the development of the Rayleigh instability will be accompanied by the decrease of the electric field profile sharpness. To derive a more founded conclusion on this topic let's use the results of quasi-linear analysis, carried out in [6]. In this work variations in the distribution of time-averaged electron plasma parameters under the influence of diocotron instability development are considered using standard quasi-linear techniques. Since, as noted above, equation (6) is the exact copy of the equation, describing diocotron instability development, the results of the analysis carried out in [6] are applicable in our case. Not repeating consecutive computations, analogous to those given in [6], let's write down only the final result. In the

lowest nonlinear approximation, when only the reverse influence of the perturbations on the time-averaged parameters is taken into account, we come to a parabolic ("diffusion") equation

$$\frac{\partial}{\partial t} < u_y > (x,t) = D \frac{\partial^2 < u_y > (x,t)}{\partial x^2} \qquad (8),$$

where

$$< u_y > (x,t) = -\frac{< E > (x,t)}{B_0} = \frac{1}{B_0} \frac{\partial}{\partial x} < \Phi > (x,t) \qquad (9)$$

$$< \Phi > (x,t) = \frac{k}{2\pi} \int_0^{\frac{2\pi}{k}} \Phi(x,y,t) dy \qquad (10).$$

$<u_y>(x,t)$ represents the value of the electron drift velocity averaged over the azimuth wavelength component $<u_y>(x,0)=u_0(x)$; $<E>(x,0)=E_0(x)$.

The "diffusion" coefficient $D = \frac{2}{\varepsilon_0 B_0^2} \sum_k \frac{\gamma_k \xi_k}{(\omega_k - k < u_y >)^2 + \gamma_k^2}$, (11),

where ω_k, γ_k – correspondingly the real part of the frequency and the increment of the instability of mode with wave number k.

$$\xi_k = \frac{\varepsilon_0 k^2 |\Phi_k'|^2}{2} \qquad (12),$$

$$\Phi_k'(x,t) = \frac{\Phi(x,y,t) - < \Phi > (x,t)}{e^{iky}} \qquad (13).$$

ξ_k is defined from the equation:

$$\frac{\partial \xi_k}{\partial t} = 2\gamma_k \xi_k \qquad (14)$$

ω_k and γ_k are found from the equation (6) substituting the current value $<u_y>$, defined from the equation (8) instead of u_0.

Having the original profile of drift velocity $u_0(x)$ and setting the initial value of potential perturbation amplitude we can, by means of solving self-consistent system of equations (6), (8)-(14), find the profile of the drift velocity and the perturbation amplitude change in the course of time. In the present work we will not do that; instead we will use equation (8) only for qualitative analysis of the initial perturbation relaxation process. Since the diffusion coefficient (11) is positive, the sign of the time derivative $\frac{\partial}{\partial t} < u_y > (x,t)$ is defined by the second coordinate x derivative of $<u_y>$. In Fig.2 the part of drift velocity profile (in HT acceleration channel) with the point of inflection is shown. As it was marked above, the necessary condition of instability is the presence of the point of inflection, which is always satisfied for the real drift velocity profiles in channel. By definition, as the second derivative, $\frac{\partial^2 < u_y > (x,t)}{\partial x^2}$, passes the point of inflection it should change its sign. To the left side of this point the second derivative will be positive, to the right – negative. It means that if in the initial moment the drift velocity profile looked like it was shown in Fig.2 by the solid line, then after some time it will change in a following way: the drift velocity will decrease to the right of the inflection point and increase to the left, i.e. the drift velocity profile will become less sharp.(In Fig.2, the new profile is presented by the dotted line.) Therefore, the electric field profile, which is connected with $<u_y>$ linearly, also will become less sharp. At the same time the discharge voltage $U_d = \int_0^t dt \int_0^d < E > (x,t) dx$ will remain unchanged.

Therefore, as a result of Rayleigh instability development, the electric field is de-localized, and therefore is decreased. Since at the same time the radial electric field, due to the radial gradient of electron pressure, remains unchanged, the structure of the electric field equipotentials in the acceleration channel becomes more defocusing. As a result, the divergence of the ion flow increases, which finally should result in unfavorable changes concerning the thruster lifetime.

4. Influence of Magnetic Field and Electron Number Density Gradients on Rayleigh Instability in HT

In work [5] on the basis of the numerical solution of the equation (6) the detailed investigation of the Rayleigh instability in HT was carried out. It was done for the conditions, when it is possible to neglect the magnetic field and electron number density non-uniformity in comparison with the electric field one. For that double-point boundary eigenvalue problem was solved using the shooting method; so-called global-converging iteration procedure of Newton-Raffson was applied. Attempts to take into account the influence of the real n_0 and B_0 gradients, i.e. to use the equation (5) were of limited success that was connected with the rapid growth of the demands to the initial approximation accuracy, i.e. to the proximity of the test values of ω_k and γ_k to the actual values. In some cases when the values of the parameter α introduces above were high and the electric field profiles were close to the nominal, the mentioned difference should not have exceeded 1% (!). During the accomplishment of the present work upon the equation (5) integration, the Runge-Kutta driver with adaptive stepwise control was changed by the Rosenbrock method for stiff systems solution. Also the algorithm of the problem solution itself was changed. In the new algorithm, the parameter α increased gradually, "step by step". On every new step the ω_k and γ_k values, obtained at the previous step, were used as initial approximation. The improvements mentioned allowed to advance in the eigenvalues problem solution up to $\alpha=1$.

The problem was solved as follows. For typical $n_0(x)$, $B_0(x)$ and $E_0(x)$ (or $u_0(x)$) distributions, for example such as the distributions shown on Fig.1, the values of ω_k, γ_k for different values of $k=m/r_0$ ($m=\pm1, \pm2, \pm3$) were found using equation (5) and boundary conditions (5'). The same way as in [5], the distributions of undisturbed parameters were specified using the approximation formula:

$$\varphi_n = \frac{1}{\frac{\sinh^2[a_n(x-c_{n)}]}{\sinh^2[a_n q_n]}+1} \qquad n=1,2,3 \qquad (15)$$

By the choice of the fitting parameters a_n, c_n, q_n , it is possible to obtain practically all distribution profiles of interest.

Taking into account the gradients of n_0, B_0 in the numerical modeling leads to the quantitative and qualitative changes in the electron perturbations properties. In Fig.3 the dependences of ω_k, γ_k (divided by $|u_{0\max}|/r_0$) for the first longitudinal harmonic and for m=-1 and m=-2 are shown vs. the β number, which characterizes the degree of non-uniformity of electron number density and magnetic field.

$$\beta = \frac{\frac{\partial}{\partial x}(\ln\frac{n_0}{B_0})}{\frac{\partial}{\partial x}(\ln\frac{n_0}{B_0})_{nom}} \qquad (16).$$

The denominator of (16) corresponds to the distribution of parameters in Fig.1. Here α=0.54. It is seen that upon the increase of β the decrease of instability increment, as well as frequency, happens, with the exception of the little area near zero, where a relative burst of these values occurs. In Fig.4 the structure of real and imaginary parts of Φ is presented for two consecutive β values. It can be seen that as the β increases, the area of Rayleigh perturbations localization reduces. They more and more concentrate in the area of the strong electric field, moving away from the boundaries. Seemingly, this fact is the physical reason of the computational difficulties upon the transit to the strongly non-uniform n_0 and B_0. In Fig.5 the dependence of ω_k, γ_k vs. the azimuth mode number is presented for β=1 and α=0.54. As it is seen from the figure, upon the increase of m absolute value the perturbations frequency in the range under consideration is continuously increasing, at the same time the instability increment at first is also increasing, and then abruptly drops.

The investigations have also shown that the increments and frequencies of Rayleigh perturbations were sensitive to details of the drift velocity profile. The latter makes possible using the RF spectrum in MHz range emitted by HT and captured by close-by antenna as a mean for non-contact diagnostics of the electric field distribution inside the thruster during flight.

5. Electron Gradient Perturbations in Hall Thrusters

Alongside with the quantitative variations in the structure of Rayleigh perturbations, the qualitative changes in electron perturbations arise, together with the transition to non-uniform n_0 and B_0. During the numerical

modeling, solutions appear which correspond to other, non-Rayleigh perturbations. In Figs. 6-7 examples of the longitudinal structure of these perturbations are presented. The perturbations can be divided into two groups. The first group includes the waves (Fig.6), which as Rayleigh perturbations, propagate in the direction of the electron drift. Their frequency is strongly dependent on the longitudinal number ***l***, rapidly decreasing upon its increase. The area of these perturbations localization approximately coincides with the area of Rayleigh perturbations, but is significantly broader.

The second group includes perturbations, which propagate in a direction opposite to the direction of electrons drift. The frequencies of these perturbations are intermediate between the frequencies of the waves from the first group and the Rayleigh perturbations, and decrease as the longitudinal number increase. As the azimuth number increases, the frequency at first grows, and then reduces. The localization of the second group perturbations differs both from the Rayleigh perturbations localization and from the waves from the first group localization (fig.7). These perturbations are localized mainly in the area between the anode and the beginning of the strong electric field area.

Before discussing the nature of the perturbations of the first and second type it is necessary to make one principal note. In contrast to the Rayleigh perturbations, these perturbations are stable in linear approximation (at least in the frames of assumptions made upon the equation (5) derivation and within the numerical computation inaccuracy, which is estimated as $10^{-3}\omega_k$). That is why at first sight these perturbations seem unimportant. However, first, they may be used for the active diagnostics of thruster working processes, namely, feeding alternating voltage to one near-wall probe and registering with the aid of other near-wall probes, spaced on the azimuth and the length of the channel, area of localization and phase velocity of mentioned perturbations, the distributions of such parameters as electric field and electron number density in the channel may be obtained. Second, as it will be discussed later in detail, these perturbations may grow as a result of non-linear interactions with the Rayleigh perturbations.

To explain the nature of the first and second group perturbations let's act the following way. First, for simplicity we set $\frac{du_0}{dx} \approx 0$. Second, we assume that on a length scale of electric potential perturbation, the non-disturbed electron number density and magnetic field variation is relatively small. Then in equation (5) we may neglect the second term in comparison with the first, and keep the term with n_0 and B_0 gradients, which includes large factor ω_{Be}. Then, let's replace the $\frac{d}{dx}$ operators, which act on Φ_k, by ik_x, and temporarily let's re-designate k by k_y (for symmetry). As a result we obtain the following local dispersion equation:

$$(\omega - k_y u_0)k_\Sigma^2 = k_y \omega_{Be} \frac{d}{dx}(\ln \frac{n_0}{B_0}) \qquad (17),$$

where $k_\Sigma^2 = k_x^2 + k_y^2$

From (17), the expression for frequency follows:

$$\omega = k_y u_0 + \frac{k_y \omega_{Be} \frac{d}{dx}(\ln \frac{n_0}{B_0})}{k_\Sigma^2} \qquad (18)$$

The expression (18) describes well-known in electron magnetohydrodynamics potential continuation of electron gradient waves (see, for example, [7]), with two differences: 1) the characteristics of this wave are described not only by the number density gradient, but also by the magnetic field gradient; 2) the wave frequency as a result of Doppler effect is shifted by the value of $k_y u_0$. For the following analysis of the electron perturbations nature let's turn to Fig.8, where the values of $\frac{d}{dx}(\ln \frac{n_0}{B_0})$ are presented for nominal parameters distribution in channel. It may be seen, that the sign of the derivative of undisturbed parameters logarithm changes from positive, in the area between the anode and the beginning of the strong electric field (let's designate this area as zone 1), to negative, in the remaining area (zone 2). In accordance with (18) and Fig.8 we have the following situations.

In zone 1

While $k_y>0$ (i.e. while $m>0$) the value of ω_k is positive at condition that

$$\frac{\omega_{Be}}{k_\Sigma^2}\frac{d}{dx}(\ln\frac{n_0}{B_0}) > |u_0| \qquad (19)$$

Here as ω_{Be}, $\frac{d}{dx}(\ln\frac{n_0}{B_0})$ and u_0 the average values on the interval under consideration should be taken. In the case that $k_y<0$ (correspondingly $m<0$), the positive values of ω_k exist at

$$|u_0| > \frac{\omega_{Be}}{k_\Sigma^2}\frac{d}{dx}(\ln\frac{n_0}{B_0}) \qquad (20)$$

In zone 2

The ω_k positive values are achieved only if $k<0$. Thus, formally in two zones three groups of electron gradient waves may exist – two with the negative value of k_y, and one with the positive value of k_y. But taking into account the smallness of average value of $|u_0|$ (see Fig.1), in zone 1, the condition (20) may be met only for fairly high values of k_Σ^2, and since the main contribution to k_Σ^2 is given by k_x^2, this condition may be met only for waves with the longitudinal wave number not less than 20. This was really unachievable in the numerical solution of the boundary eigenvalue problem and is generally oversteps the frames of the assumptions, because in this case wavelength longitudinal component is commensurable with the electron Larmor radius.

The comparison of other two groups of gradient waves with the results of numerical solution of the problem, points to their direct agreement with what observed in the course of numerical modeling. Hence we may tell that in Hall thruster upon the parameters distribution shown on Fig.1, three types of electron perturbations may occur: the Rayleigh waves (unstable already in the linear approximation) and two types of electron gradient waves: 1) in the area between the anode and the area of strong electric field – the waves propagating in the direction opposite to the direction of electrons drift; 2) in the remaining area – electron gradient waves propagating in the direction of electron drift.

6. About the Possibility of Electron Gradient Wave Excitation as a Result of Non-linear Processes

The broad oscillation spectrum, which is observed in many plasma systems, is the consequence of non-linear energy transfer from the limited number of unstable modes to other waves (which may co-exist in the particular plasma system). This effect may be realized by means of parametric resonance. As a result of the mentioned process, the waves initially presented in plasma on the level of "thermal noises" begin to grow, taking the energy from the pumping wave, and by that limiting its amplitude.

In the case of waves of different nature, the most effective energy transfer is realized as a result of so-called three-wave process, during which three waves begin interaction, and one of them is unstable in the linear approximation. The necessary condition for such process is the following:

$$\omega_0 = \omega_1+\omega_2 \qquad (21),$$

$$\mathbf{k}_0 = \mathbf{k}_1 + \mathbf{k}_2 \qquad (22).$$

As for the condition (22), in our case it is enough that the condition for the azimuth component is met*:*

$$k_{y0}=k_{y1}+k_{y2} \qquad (23),$$

since along the magnetic field line the perturbations may be regarded as infinitely stretched, i.e. k_{z1}, k_{z2}, $k_{z3}\rightarrow 0$, and along the x axis the waves are standing.

Since $k_y=m/r_0$, (23) may be replaced by the following condition:

$$m_0=m_1+m_2 \qquad (24)$$

In table 1 the examples for which the conditions (21) and (24) for the wave triplets, including both the Rayleigh waves and electron gradient waves are hold true, for the nominal mode (i.e. $\beta=1$, $\alpha=0.54$), are presented. As it is seen from the table, in the considered examples the condition (21) is met with inaccuracy, not exceeding 10%, and the condition (24) is met with zero inaccuracy. In fig.9 the longitudinal structure of interacting waves from the first triplet in Table 1 is given as an example. It is seen that the areas of the wave localization significantly overlap that creates necessary conditions for their effective interaction.

The examples presented in Table 1 do not far exhaust all possible combinations during the three-wave interaction. As a result, a fairly complicated spectrum pattern may occur.

Table 1

Wave type and the longitudinal wave number	Frequency ω_0	Azimuth mode number	Wave type and the longitudinal wave number	Frequency ω_1	Azimuth mode number	Wave type and the longitudinal wave number	Frequency ω_2	Azimuth mode number	$\frac{\omega_0}{\omega_1+\omega_2}$	$\frac{m_0}{m_1+m_2}$
Electron gradient wave (l=2)	1.40	-1	Rayleigh wave (l=1)	1.15	-2	Electron gradient wave (l=3)	0.18	+1	0.95	1
Electron gradient wave (l=1)	3.64	+2	Electron gradient wave (l=1)	2.76	+3	Rayleigh wave (l=1)	0.54	-1	0.91	1
Electron gradient wave (l=1)	5.65	-1	Electron gradient wave (l=1)	3.64	+2	Rayleigh wave (l=1)	1.46	-3	0.9	1

7. Experimental Validation of the Theoretical Model of Electron Perturbations in HT

The straightforward and maybe the best method to validate experimentally the theoretical model of electron perturbations in HT, presented above, is to carry out correlation measurements of the spatial structure of the waves in the range of 0.5-50 MHz. However, this method would require insertion of a large number of near-wall electric probes, distributed both azimuthally (3-4 probes) and longitudinally (3-4 probes), into the acceleration channel. Therefore, the measurement of amplitude-frequency characteristics of the wave by an antenna, placed outside the acceleration channel, seems to be more preferable. One or more antennae, at different orientations and/or placed at different locations inside the vacuum chamber, should pick up electromagnetic waves generated by the alternating electric currents of the perturbations. We could look then for the dependence of the frequency of the considered wave on relatively easy controlled parameters, such as the magnetic induction strength or the average electric field value in the acceleration channel. The last parameter may be considered as proportional to the discharge voltage, at least if it does not change very much. The dependence of the wave amplitude variation on the variation of the magnetic induction and electric field values may be used as well to validate the theory. Moreover, the use of a Soreq laboratory model thruster of a modular and flexible design, allowing changes in channel geometry and magnetic circuit configuration [8,9], will enable to investigate the dependencies on the magnetic induction and electric field profiles too.

In Figs.10 and 11 the dependencies of the Rayleigh and electron gradient perturbations frequencies (divided by 2π) vs. the corresponding magnetic field induction and electric field deviations from the nominal value are presented. In the same figures the dependence of the instability increment vs. the mentioned parameters is given. It is seen that the frequencies of the electron gradient and Rayleigh perturbations react differently to the magnetic and electric field variations. This fact significantly facilitates the identification of considered perturbations. It should be noted also, that if electron gradient waves are excited as a result of nonlinear three-wave process, then variation of magnetic or electric field may lead to the breaking of resonance (21), or, vice versa, to its more exact realization. That, in turn, will promote either the reduction of electron gradient waves amplitudes or their growth.

An experiment to validate the theoretical model of electron perturbations in HT, such as described above, is being prepared at the Soreq test facility using laboratory and/or engineering model thrusters operating at the sub-kilowatt power range. The preparations include studies of appropriate antennae and their proper location and orientation, and of the electromagnetic effect of the test chamber.

8. Conclusions

1. A theoretical model of large-scale electron perturbations in Hall thruster has been developed.
2. In the frame of the theoretical model, using numerical modeling and analytical estimations it was shown that electron potential perturbations of two types may occur in the thruster – Rayleigh and Doppler shifted electron gradient.
3. Rayleigh perturbations are unstable already in linear approximation. They exist and grow owing to the specific electric drift non-uniformity in acceleration channel. It was shown, that real electron number density and magnetic field non-uniformities substantially influence the localization and the growth rate of these perturbations.

4. It was shown, that the development of the Rayleigh electron instability in HT should be accompanied by the smoothing of electric field profile in acceleration channel that leads to the limitation of its maximal reachable value. This should result finally in the increase of the ion flow divergence.
5. It was shown that increasing the gradient or/and absolute value of the magnetic field induction is the effective way to reduce the increment of Rayleigh instability and finally the amplitude of the wave.
6. Electron gradient waves, depending on localization in acceleration channel, may be running both in the direction of the electron drift and in the opposite direction, which is related to the different signs of electron number density and magnetic field gradients in different parts of acceleration channel.
7. Electron gradient waves may be excited parametrically in the plasma of the thruster, as a result of non-linear three-wave process with the aid of Rayleigh mode.
8. The analysis of characteristics of electron perturbations in Hall thruster acceleration channel may provide information about the real electric field distribution in it that is difficult to obtain by other means, especially in flight experiments.
9. For theoretical model experimental validation and refinement it is possible to use the specific character of Rayleigh and electron gradient perturbations frequency dependence vs. relatively easy controlled parameters as the discharge voltage and the magnetic field induction.
10. An experiment to validate the theoretical model is being prepared at the Soreq test facility using laboratory and/or engineering model thrusters operating at the sub-kilowatt power range.

References

1. Shishkin, G.G., Gerasimov, V.P. Plasma Instabilities in Accelerators with Closed Electron Drift, *Journ. Tech. Phys*., v.45, no.9, pp.1847-1854 (1975).
2. Shishkin, G.G. Instabilities of Plasma Perturbations in Non-uniform Plasma of Accelerators with Closed Electron Drift, in book: Sources and Accelerators of Plasma, Kharkov, KhAI, pp.14-22 (1978).
3. Vakhnuk, S.P., Kapulkin, A.M., Maslennikov, M.A., Prisnyakov, V.F. Feedback Stabilization of Plasma Instabilities in Stationary Plasma Thrusters, 2-nd German-Russian Conference on Electric Propulsion Engines and Their Technical Applications, Moscow, Preprint 5p. (1993).
4. Kapulkin, A.M., Prisnyakov, V.F. Dissipative Method of Suppression of Electron Drift Instability in SPT, Proceedings of the 24-th International Electric Propulsion Conference, IEPC-95-37, Moscow, pp.302-306 (1995).
5. Kapulkin A., Kogan A., Guelman M., Noncontact Emergency Diagnostics of Stationary Plasma Thruster in Flight, 52-nd International Astronautical Congress, Toulouse, Preprint 11 p. (2001). To be published in *Acta Astronautica*.
6. Davidson R.C., Quasilinear Theory of the Diocotron Instability for Nonrelativistic Non-neutral Electron Flow in Planar Geometry, Phys. Fluids, vol.28, no.6, pp.1937-1947 (1985).
7. Kuvshinov B.N., Rem J., Schep T.J. and Westerhoz E., Electron Vortices in Magnetized Plasmas, *Physics of Plasmas*, vol. 8, pp. 3232-3250, (2001).
8. Ashkenazy J., Raitses Y and Appelbaum G., Parametric Studies of the Hall Current Plasma Thruster, *Physics of Plasmas,* vol. 5, pp. 2055-2063, May 1998.
9. Raitses, Y., Ashkenazy, J. and Appelbaum, G., Probe Measurements of Plasma Properties Inside an Experimental Hall Thruster, AIAA-98-3640, 34th Joint Propulsion Conference, Cleveland, OH, July 1998.

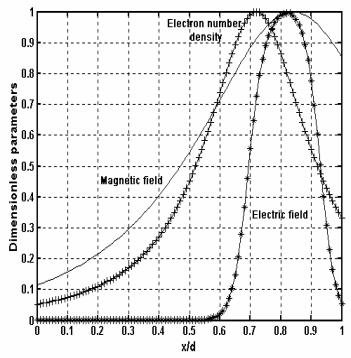

Fig.1. *Distributions of parameters in HT*

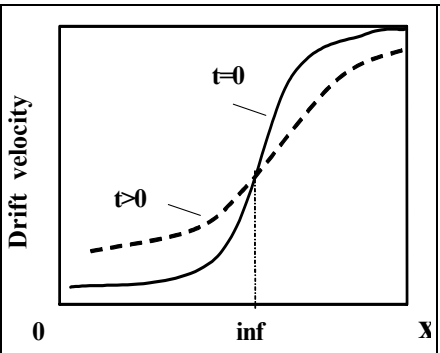

Fig.2 *Influence of Rayleigh instability on drift velocity distribution*

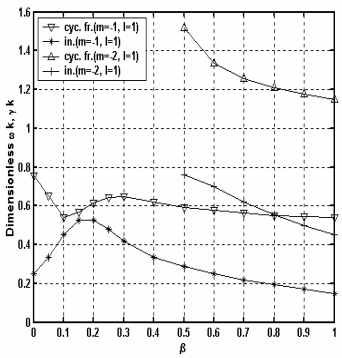

Fig.3.*Dependence of dimensionless* ω_k, γ_k *on* β

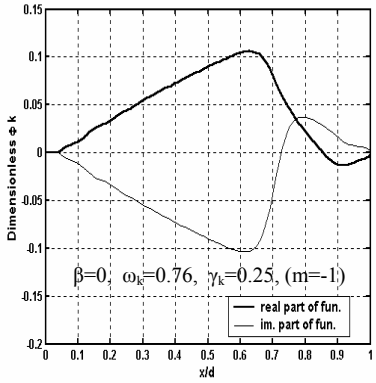

Fig.4a. *Influence of β on structure of Φ_k in channel*

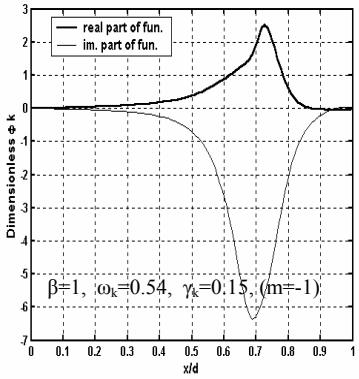

Fig.4b. *Influence of β on structure of Φ_k in channel*

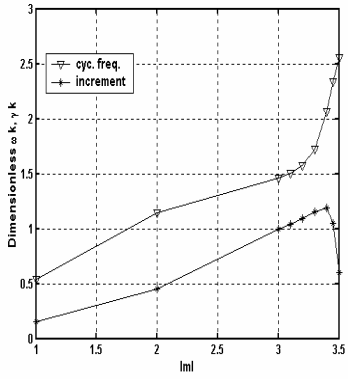

Fig.5. *Dependence of ω_k, γ_k* on lml

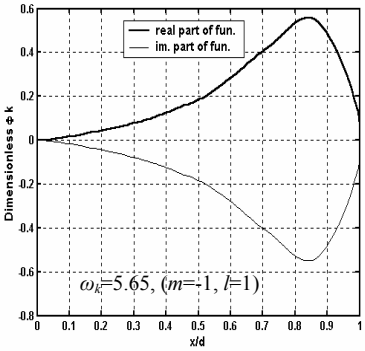

Fig.6.*Localization of electron gradient wave of first type*

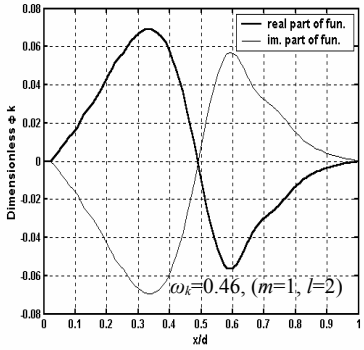

Fig.7.*Localization of electron gradient wave of second type*

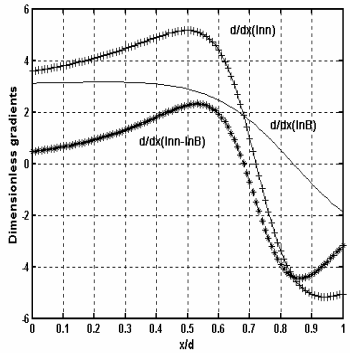

Fig.8.*Distributions of dimensionless gradients of n_0 and B_0*

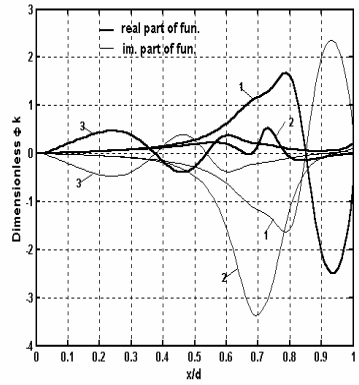

1-e.g.w.(m=-1,l=2); *2-R.w.*(m=-2, l=1); *3-e.g.w.*(m=1,l=3)

Fig.9.*Three waves interaction*

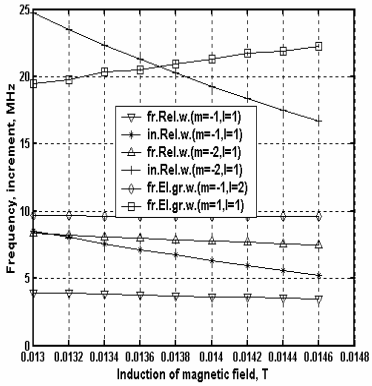

Fig.10.*Influence of B_0 on parameters of electron waves*

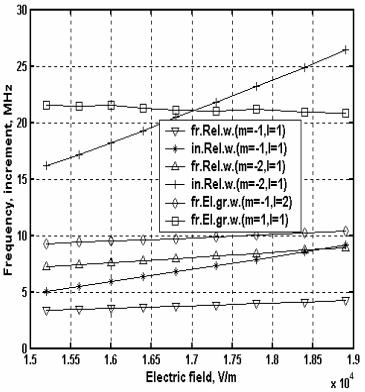

Fig.11.*Influence of E_0 on parameters of electron waves*